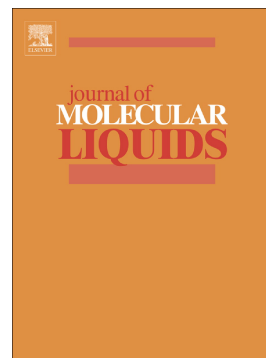


Hydrophilic role of deep eutectic solvents for clean synthesis of biphenyls over a magnetically separable Pd-catalyzed Suzuki-Miyaura coupling reaction

Mahsa Niakan, Majid Masteri-Farahani, Sabah Karimi, Hemayat Shekaari



PII: S0167-7322(20)37320-7

DOI: <https://doi.org/10.1016/j.molliq.2020.115078>

Reference: MOLLIQ 115078

To appear in: *Journal of Molecular Liquids*

Received date: 15 September 2020

Revised date: 25 November 2020

Accepted date: 12 December 2020

Please cite this article as: M. Niakan, M. Masteri-Farahani, S. Karimi, et al., Hydrophilic role of deep eutectic solvents for clean synthesis of biphenyls over a magnetically separable Pd-catalyzed Suzuki-Miyaura coupling reaction, *Journal of Molecular Liquids* (2020), <https://doi.org/10.1016/j.molliq.2020.115078>

This is a PDF file of an article that has undergone enhancements after acceptance, such as the addition of a cover page and metadata, and formatting for readability, but it is not yet the definitive version of record. This version will undergo additional copyediting, typesetting and review before it is published in its final form, but we are providing this version to give early visibility of the article. Please note that, during the production process, errors may be discovered which could affect the content, and all legal disclaimers that apply to the journal pertain.

Hydrophilic role of deep eutectic solvents for clean synthesis of biphenyls over a magnetically separable Pd-catalyzed Suzuki-Miyaura coupling reaction

Mahsa Niakan ^{a,b}, Majid Masteri-Farahani ^{a,b,*}, Sabah Karimi ^c, Hemayat Shekaari ^c

^a Faculty of Chemistry, Kharazmi University, Tehran, Iran

^b Research Institute of Green Chemistry, Kharazmi University, Tehran, Iran

^c Department of Physical Chemistry, Faculty of Chemistry, University of Tabriz, Tabriz, Iran

E-mail address: mfarahani@khu.ac.ir

Abstract

The development of an efficient and sustainable catalytic system for the preparation of biphenyls through the Suzuki-Miyaura coupling reaction is still a great challenge to green chemistry. Encouraging the prevailing challenge, in the present work, a heterogeneous Pd catalyst was synthesized through a green method and used for the production of biphenyls in deep eutectic solvents (DESs) as green reaction media. In order to prepare the catalyst, magnetite-graphene oxide nanocomposite was modified with cellulose via the click reaction and applied as support for Pd nanoparticles. Cellulose acted as both reducing and stabilizing agent for Pd nanoparticles and eliminated the requirement of a reducing agent. The prepared catalyst was characterized by different methods such as FT-IR, EDX, EDX-mapping, XPS, SEM, TEM, XRD, VSM, and ICP-OES analyses. Catalytic properties of the obtained catalyst was explored in the coupling reaction of aryl halides with aryl boronic acids in different hydrophilic and hydrophobic DESs. The presence of cellulose with hydrophilic character on the structure of catalyst offered well dispersion of the catalyst in hydrophilic DESs, which led to enhancement of its catalytic activity. Among various hydrophilic DESs, the DES composed of dimethylammonium chloride and

glycerol was verified as the most effective solvent for the preparation of biphenyls. The catalyst was compatible with a variety of substrates, with which all the Suzuki coupling products were achieved in high to excellent yields. Thanks to the low solubility of catalyst and DES in organic solvents, the separated aqueous phase containing both of the catalyst and DES could be readily recovered by evaporating water and reused up to five successive runs with a stable activity. This simple and new separation strategy provided a clean and highly efficient synthetic methodology for the synthesis of various biphenyls. Moreover, hot filtration test efficiently confirmed that the catalyst is heterogeneous and completely stable under reaction conditions.

Keywords: Cellulose; Magnetite-graphene oxide nanocomposite; Pd catalyst; Click reaction; Suzuki-Miyaura reaction; Deep eutectic solvent.

1. Introduction

The catalytic cross-coupling reaction between organoboronic acids and aryl halides in the presence of palladium (Pd) compounds is a powerful tool for the synthesis of biphenyl structures as essential feedstocks for the production of pharmaceuticals, natural products, polymers, and agrochemicals [1-3]. Compared to homogeneous Pd catalysts, heterogeneous counterparts have been accepted as environmentally friendly alternatives owing to their better recoverability and easier separation [4,5]. In this regard, the homogeneous Pd catalysts have been immobilized on various solid supports making them heterogeneous in nature [6-8]. Recently, cellulose has received significant attention as support for developing heterogeneous Pd catalyst systems owing to its outstanding properties such as abundant availability, non-toxicity, biodegradability, environmental friendly, and low cost [9-15]. Also, abundant hydroxyl groups in cellulose backbone can act as both reducing and stabilizing agents for many metal nanoparticles and therefore eliminate the requirement of a reducing agent or stabilizer [16,17]. However, the

separation and recycling of cellulose-based Pd catalysts is challenging due to the dispersion stability of cellulose in different solvents [18]. Consequently, the development of novel routes for the synthesis of cellulose-based Pd catalysts with good recyclability is still necessary. Modification of easily separable magnetic graphene oxide nanocomposite with cellulose is an effective approach to prepare a versatile and promising support for immobilization of Pd catalysts [19,20]. Among the numerous methods for the modification of magnetic graphene oxide nanocomposite, the azide-alkyne cycloaddition in the presence of copper as catalyst is an attractive modification method and offers several advantages including high yields and selectivity under mild conditions [21,22].

Over the past few decades, researchers were encouraged to develop cleaner processes as alternatives to traditional chemical syntheses and transformations by the application of environmentally friendly solvents [23-25]. Currently, the utilization of deep eutectic solvents (DESs) as reaction media has attracted a growing attention in organic syntheses. They are eco-friendly liquids obtained by reacting a hydrogen bond acceptor and a hydrogen bond donor, which self-associate via reciprocal hydrogen-bonding to form a new eutectic phase with a melting point below those of the initial components [26]. Compared to common organic solvents, DESs are cheap, renewable, easy to prepare and recycle, biodegradable, and non-toxic [27,28]. Therefore, they have made a remarkable impact on clean synthesis in recent years. Although DESs are favorable green solvents, the application of DESs in Suzuki- Miyaura coupling reaction is in its infancy and only a few works have been reported to date [29-34].

From the foregoing, we decided to prepare a novel heterogeneous catalyst with immobilizing Pd nanoparticles on clicked cellulose-modified magnetite-graphene oxide nanocomposite and

investigate its catalytic properties in the Suzuki-Miyaura coupling reaction in DESs as sustainable and environmentally benign reaction media for the clean synthesis of biphenyls.

2. Experimental

2.1. Catalyst preparation

2.1.1. Preparation of azide-functionalized $\text{Fe}_3\text{O}_4/\text{GO}$ ($\text{Fe}_3\text{O}_4/\text{GO}@\text{N}_3$)

GO was synthesized from graphite by a modified Hummers method as described elsewhere [35]. Magnetite-graphene oxide nanocomposite ($\text{Fe}_3\text{O}_4/\text{GO}$) was synthesized by using a co-precipitation method according to the literature procedure [35]. $\text{Fe}_3\text{O}_4/\text{GO}$ (1.0 g) was uniformly dispersed into 40 mL of dry toluene with the help of ultrasound for 30 min. Afterwards, 3-chloropropyltriethoxysilane (3-CPTES, 3 mL) was added and the reaction mixture was refluxed for 24 h under nitrogen gas. The obtained $\text{Fe}_3\text{O}_4/\text{GO}@\text{Cl}$ was isolated from the reaction mixture with applying the magnet and rinsed repeatedly with ethanol before being vacuum dried at 80 °C for 8 h. Then, 1.0 g of $\text{Fe}_3\text{O}_4/\text{GO}@\text{Cl}$ was ultrasonically dispersed in a solution containing 2.0 g of NaN_3 in 50 mL of dimethylformamide (DMF) and the mixture was stirred at 80 °C for 10 h. The obtained precipitate was collected magnetically, rinsed with DMF, and vacuum dried at 80 °C for 12 h to give $\text{Fe}_3\text{O}_4/\text{GO}@\text{N}_3$.

2.1.2. Preparation of alkyne-functionalized cellulose

Alkyne-functionalized cellulose was synthesized based on the previously reported procedure [37]. 1.0 g of cellulose was suspended in 100 mL of basic aqueous solution (1.1 wt % NaOH) at room temperature for 1 h to allow it swell sufficiently and increase the accessibility of hydroxyl groups to chemical reagents. The reaction medium was progressively heated up to 60 °C over 1 h and then the required quantity of propargyl bromide was rapidly added. After stirring at 60 °C

for 24 h, the mixture was filtered and washed with ethanol and water. After drying at 60 °C, alkyne-functionalized cellulose was obtained and characterized by FT-IR spectroscopy (Figure S1).

2.1.3. Preparation of cellulose-modified Fe₃O₄/GO via click reaction (Fe₃O₄/GO@CL)

Click reaction was applied to conjugate the alkyne-functionalized cellulose with Fe₃O₄/GO@N₃. Briefly, a mixture of well dispersed Fe₃O₄/GO@N₃ (1.0 g), alkyne-functionalized cellulose (2.0 g), copper (II) sulfate (0.1 g), and sodium ascorbate (2.0 g) in 60 mL of dry DMF was stirred at 50 °C for 24 h. After cooling the reaction mixture to ambient temperature, the product was isolated with the help of a magnet. It was rinsed with DMF and deionized water before vacuum drying at 80 °C for 12 h.

2.1.4. Immobilization of Pd nanoparticles on Fe₃O₄/GO@CL

Palladium acetate (0.5 mmol, 0.11 g) was added into a mixture of Fe₃O₄/GO@CL (1.0 g) in 50 mL of absolute ethanol and ultrasonicated for 30 min. After stirring for 24 h at room temperature, the black product was isolated by an external magnet, rinsed with ethanol, and vacuum dried at 80 °C for 6 h to afford Fe₃O₄/GO@CL-Pd.

2.2. Preparation of DESs

DESs were synthesized according to the previously described procedure [38-40]. In brief, a mixture of hydrogen bond donor (HBD) and hydrogen bond acceptor (HBA) with the molar ratio given in Table 1 was stirred at given temperature until a colorless solution was achieved.

Table 1. Synthesis parameters for DESs.

| DES | HBA | HBD | Molar ratio | T (°C) |
|-----|-----|-----|-------------|--------|
|-----|-----|-----|-------------|--------|

| | | | | |
|-----------|---------------------------------|---------------|-----|----|
| ChCl:Urea | Choline chloride | Urea | 1:2 | 70 |
| ChCl:CA | Choline chloride | Citric acid | 1:1 | 80 |
| ChCl:MA | Choline chloride | Malonic acid | 1:1 | 80 |
| ChCl:Gly | Choline chloride | Glycerol | 1:2 | 80 |
| DMAC:Urea | Dimethylammonium chloride | Urea | 1:2 | 80 |
| DMAC:CA | Dimethylammonium chloride | Citric acid | 1:2 | 80 |
| DMAC:MA | Dimethylammonium chloride | Malonic acid | 1:2 | 80 |
| DMAC:Gly | Dimethylammonium chloride | Glycerol | 1:2 | 80 |
| TBAB:OA | Tetrabutylammonium bromide | Octanoic acid | 1:2 | 90 |
| TBAB:DA | Tetrabutylammonium bromide | Decanoic acid | 1:2 | 90 |
| TOMAC:OA | Trioctylmethylammonium chloride | Octanoic acid | 1:2 | 90 |
| TOMAC:DA | Trioctylmethylammonium chloride | Decanoic acid | 1:2 | 90 |

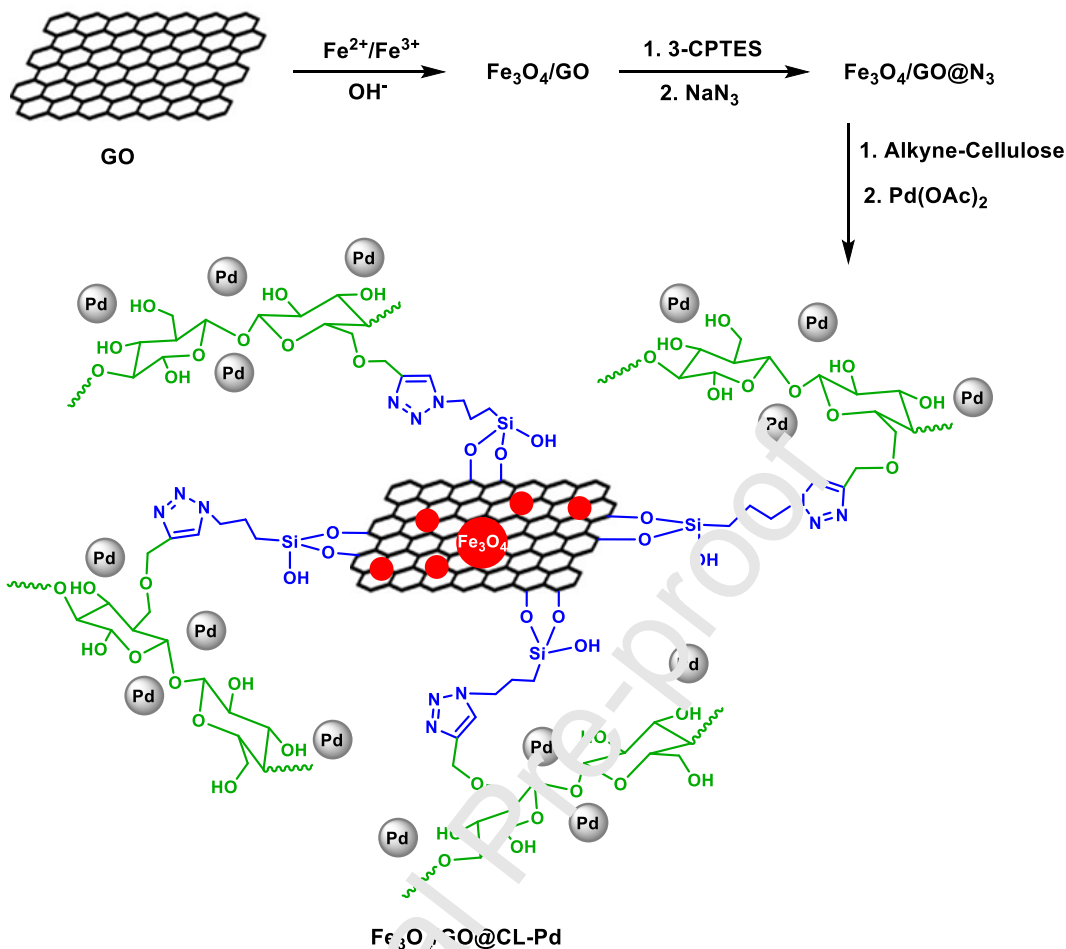
2.3. Suzuki-Miyaura cross-coupling reaction in the presence of Fe₃O₄/GO@CL-Pd

A mixture of aryl boronic acid (1.1 mmol), aryl halide (1.0 mmol), K₂CO₃ (2.0 mmol), and Fe₃O₄/GO@CL-Pd (0.005 g, 0.01 mol%) in 3 mL of DES (DMAC:Gly) was stirred at 80 °C for given time. The extent of reaction was checked using thin layer chromatography. At the end of reaction, the mixture diluted with 15 mL of water and extracted with ethyl acetate (3 × 10 mL). After removing the volatiles from the organic fraction, the residue was purified by column chromatography on silica gel with an eluent consisting of ethyl acetate and n-hexane to achieve the desired product. The products were characterized by ¹H NMR and melting point followed by comparison with authentic standard samples. The aqueous phase, which contained both of the catalyst and DES, was used for another run after evaporation of water.

3. Results and discussion

3.1. Preparation and characterization of Fe₃O₄/GO@CL-Pd

The catalyst was prepared according to the synthetic route described in Scheme 1. GO was first prepared via modified Hummers method and then modified with magnetite nanoparticles to achieve Fe₃O₄/GO. Afterwards, Fe₃O₄/GO was organo-functionalized by the condensation reaction of 3-CPTES and hydroxyl groups on the surface of Fe₃O₄/GO, followed by the substitution reaction of chloro groups with azide ions to produce Fe₃O₄/GO@N₃. The prepared Fe₃O₄/GO@N₃ was subsequently reacted with pre-synthesized alkyne functionalized cellulose to give Fe₃O₄/GO@CL through click reaction. Finally, treatment of Fe₃O₄/GO@CL with Pd(OAc)₂ in absolute ethanol provided the desired catalyst (Fe₃O₄/GO@CL-Pd). Based on inductively coupled plasma optical emission spectroscopy (ICP-OES) analysis, the amount of Pd loaded on Fe₃O₄/GO@CL-Pd was found to be 0.41 mmol.g⁻¹.



Scheme 1. Synthetic route for the preparation of $\text{Fe}_3\text{O}_4/\text{GO}@CL\text{-Pd}$.

Qualitative identification of functional groups present in the products formed in each step was performed by recording FT-IR spectra (Figure 1). The peaks at 3400, 1715, 1607, 1225, and 1052 cm^{-1} in the FT-IR spectrum of GO can be attributed to the stretching vibrations of O-H, C=O, C=C, C-O-H, and C-O-C epoxy groups, respectively [41]. The formation of $\text{Fe}_3\text{O}_4/\text{GO}$ nanocomposite was affirmed by the observation of two peaks at 510 and 630 cm^{-1} due to the Fe-O stretching vibrations in Fe_3O_4 nanoparticles [42]. A new peak at 2175 cm^{-1} in the spectrum of $\text{Fe}_3\text{O}_4/\text{GO}@N_3$, was due to the stretching vibration of azide ($-N_3$) groups, verifying their attachment on the surface of $\text{Fe}_3\text{O}_4/\text{GO}$. Besides, the peaks observed at $2800\text{-}3000 \text{ cm}^{-1}$ was assigned to the stretching vibrations of the alkyl chains (C-H) in silylating agent. However, the

characteristic peak of azide groups at 2000-2200 cm^{-1} was eliminated in the spectrum of $\text{Fe}_3\text{O}_4/\text{GO}@CL$ upon formation of triazole rings during the click reaction of $\text{Fe}_3\text{O}_4/\text{GO}@N_3$ with alkyne-functionalized cellulose. Such changes have also been observed by other researchers [43,44]. In parallel, the intensity of O-H stretching vibrations at 3420 cm^{-1} increased significantly because of the presence of abundant hydroxyl groups in cellulose structure. The results clearly confirmed the successful attachment of cellulose to $\text{Fe}_3\text{O}_4/\text{GO}$ via click reaction. The spectrum of $\text{Fe}_3\text{O}_4/\text{GO}@CL\text{-Pd}$ exhibited almost no change after immobilization of Pd nanoparticles on the surface of $\text{Fe}_3\text{O}_4/\text{GO}@CL$.

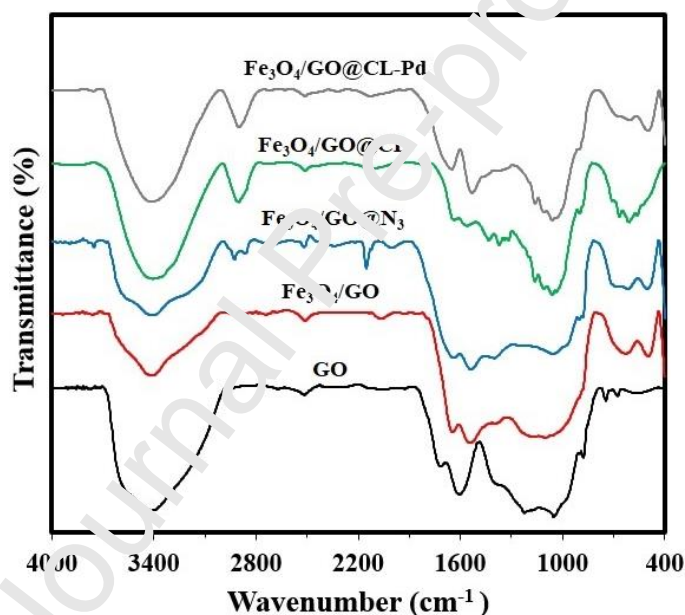


Figure 1. FT-IR spectra of GO, $\text{Fe}_3\text{O}_4/\text{GO}$, $\text{Fe}_3\text{O}_4/\text{GO}@N_3$, $\text{Fe}_3\text{O}_4/\text{GO}@CL$, and $\text{Fe}_3\text{O}_4/\text{GO}@CL\text{-Pd}$.

Energy dispersive X-ray (EDX) analysis was done to explore the surface chemical composition of the catalyst. All the expected elements C, N, O, Si, Fe, and Pd were observed in the EDX spectrum of $\text{Fe}_3\text{O}_4/\text{GO}@CL\text{-Pd}$ (Figure 2). Furthermore, the homogeneous dispersion of these elements throughout the catalyst surface was demonstrated by the corresponding EDX elemental mapping images of $\text{Fe}_3\text{O}_4/\text{GO}@CL\text{-Pd}$ (Figure S2).

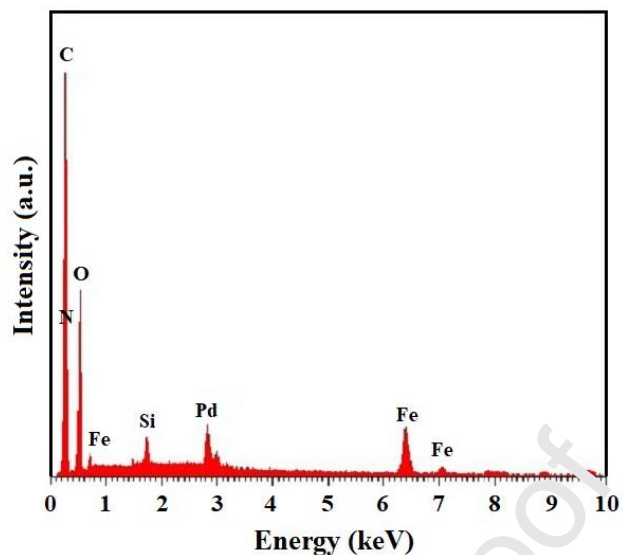


Figure 2. EDX spectrum of $\text{Fe}_3\text{O}_4/\text{CO}@CL\text{-Pd}$.

To further elucidate the chemical composition of the catalyst, X-ray photoelectron spectroscopy (XPS) was conducted as exhibited in Figure 3. The full XPS spectrum of $\text{Fe}_3\text{O}_4/\text{GO}@CL\text{-Pd}$ exhibited peaks for Si 2s, Si 2p, C 1s, Fe 3d, N 1s, O 1s, and Fe 2p, which approved the successful synthesis of the catalyst. The high-resolution XPS spectrum of Pd 3d showed doublet peaks at the binding energies of 335.67 and 341.18 eV due to Pd $3d_{5/2}$ and Pd $3d_{3/2}$, respectively, confirming the zero oxidation state of Pd [45]. Additionally, no peaks corresponding to the Pd^{2+} oxidation state were found, indicating the efficient reduction of the Pd^{2+} ions into metallic Pd nanoparticles during the catalyst synthesis. From these results, it can be concluded that cellulose component not only reduced the Pd^{2+} ions but also stabilized Pd nanoparticles and prevented from their oxidation.

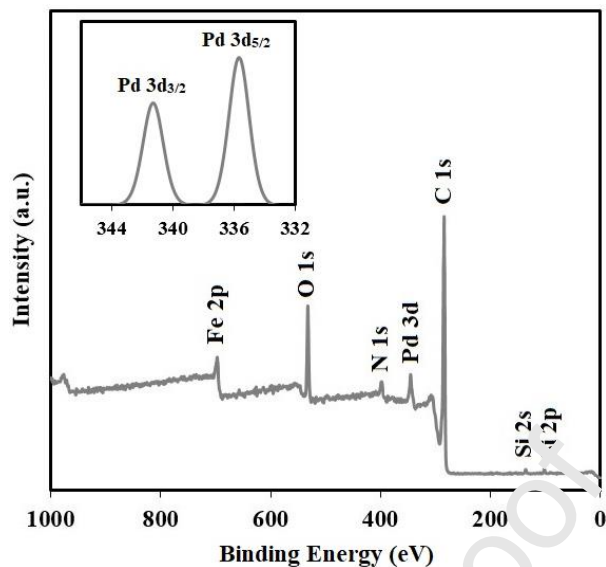


Figure 3. XPS spectrum of $\text{Fe}_3\text{O}_4/\text{GO}@CL\text{-Pd}$. Inset: high-resolution XPS spectrum of Pd 3d core-level.

The morphologies and structures of the prepared materials were studied by scanning electron microscopy (SEM) method and the images were presented in Figure 4. The pristine GO had a transparent, wrinkled, and lamellar morphology (Figure 4a). Compared to the pristine GO, $\text{Fe}_3\text{O}_4/\text{GO}$ (Figure 4b) showed the presence of Fe_3O_4 nanoparticles on the surface of GO nanosheets, which was consistent with previous reports [46,47]. As can be seen in Figure 4c, $\text{Fe}_3\text{O}_4/\text{GO}@CL\text{-Pd}$ also exhibited a similar morphology to $\text{Fe}_3\text{O}_4/\text{GO}$.

Transition electron microscopy (TEM) technique was employed for further investigation of the structural properties of the prepared samples and the results were depicted in Figure 4. The layered and sheet-like structure characteristic of GO structure was seen in the TEM image of the pristine GO (Figure 4d). After incorporation of magnetite, Fe_3O_4 nanoparticles with diameter of 8-10 nm and spherical morphology were well distributed on the surface of GO nanosheets without obvious aggregation as illustrated in the TEM image of $\text{Fe}_3\text{O}_4/\text{GO}$ (Figure 4e). The TEM image of $\text{Fe}_3\text{O}_4/\text{GO}@CL\text{-Pd}$ (Figure 4f) revealed that the structure and morphology of $\text{Fe}_3\text{O}_4/\text{GO}$ nanocomposite was well retained during the synthesis of the catalyst.

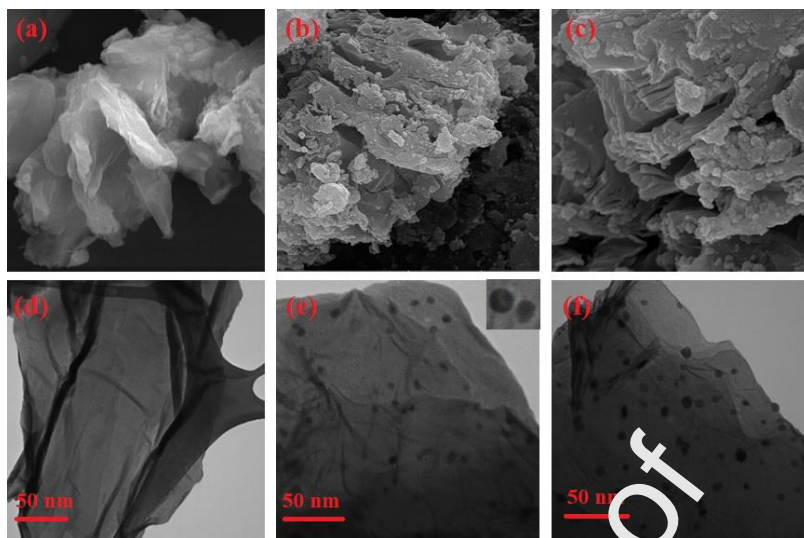


Figure 4. SEM images of (a) GO, (b) $\text{Fe}_3\text{O}_4/\text{GO}$, and (c) $\text{Fe}_3\text{O}_4/\text{GO}@CL\text{-Pd}$, and TEM images of (d) GO, (e) $\text{Fe}_3\text{O}_4/\text{GO}$, and (f) $\text{Fe}_3\text{O}_4/\text{GO}@CL\text{-Pd}$.

The X-ray diffraction (XRD) patterns of GO and $\text{Fe}_3\text{O}_4/\text{GO}@CL\text{-Pd}$ were recorded to explore their crystalline structures (Figure 5). A relatively strong diffraction peak at $2\theta = 11.3^\circ$ corresponding to (001) plane was observed for GO which disappeared in $\text{Fe}_3\text{O}_4/\text{GO}@CL\text{-Pd}$, likely owing to the incorporation of magnetite nanoparticles between the nanosheets of GO. Similar phenomenon have also been reported by other researchers preparing magnetite-graphene oxide nanocomposite [48]. The XRD pattern of $\text{Fe}_3\text{O}_4/\text{GO}@CL\text{-Pd}$ exhibited peaks at $2\theta = 30^\circ$, 35° , 43° , 53° , 57° , and 65° that were associated with the reflections of the (220), (311), (400), (422), (511), and (440) planes of Fe_3O_4 with face centered cubic structure (JCPDS Card no. 19-0629) [49]. Also, the peaks detected at 40° , 46° , and 67° which corresponded to the (111), (200), and (220) planes of metallic Pd, definitely indicated the successful reduction of the Pd^{2+} ions into Pd nanoparticles [45]. The XRD peaks of Pd nanoparticles appeared in very low intensity. Such a feature, which was also reported by other research groups [50,51], can be due to the small size of Pd nanoparticles and their well-dispersion on the surface of $\text{Fe}_3\text{O}_4/\text{GO}@CL$.

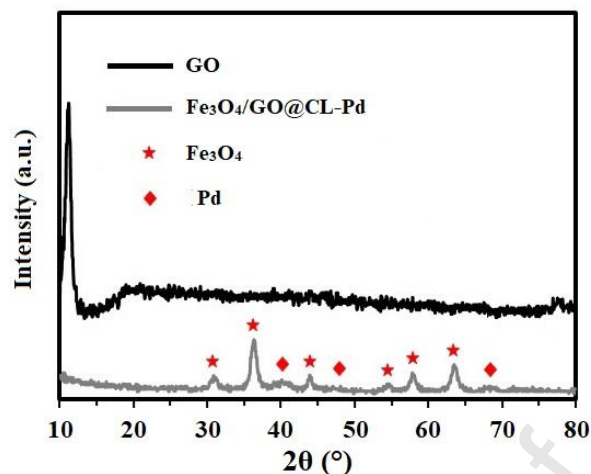


Figure 5. XRD patterns of GO and Fe₃O₄/GO@CL-Pd.

The magnetic properties of Fe₃O₄/GO and Fe₃O₄/GO@CL-Pd were evaluated by vibrating sample magnetometry (VSM). As depicted in Figure 5, neither coercivity nor remanence was observed in the magnetization curves of both samples, indicating their superparamagnetic behavior. The saturation magnetization (M_s) value of Fe₃O₄/GO@CL-Pd (19.8 emu g⁻¹) was lower than that of Fe₃O₄/GO (37.1 emu g⁻¹) owing to the less magnetic source component (Fe₃O₄) per gram in the catalyst. Nevertheless, the catalyst still possessed high magnetic response and could be efficiently separated from a solution with the help of a magnet (inset photograph in Figure 6).

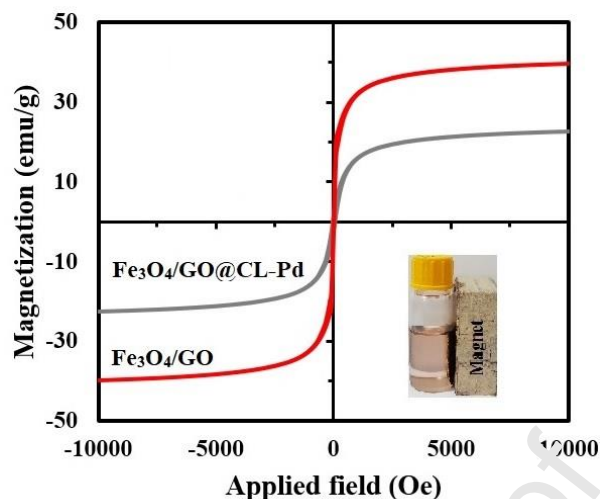


Figure 6. Magnetization curves of $\text{Fe}_3\text{O}_4/\text{GO}$ and $\text{Fe}_3\text{O}_4/\text{GO}@CL\text{-Pd}$.

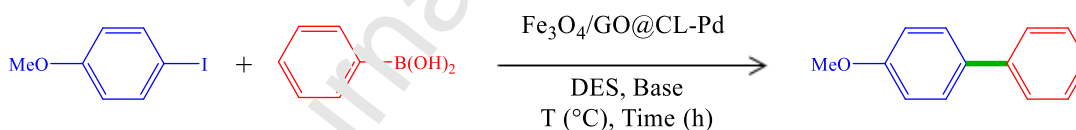
3.2. Catalytic performance of $\text{Fe}_3\text{O}_4/\text{GO}@CL\text{-Pd}$ in the Suzuki-Miyaura cross-coupling reaction

After complete characterization of $\text{Fe}_3\text{O}_4/\text{GO}@CL\text{-Pd}$, its catalytic efficiency was explored in the preparation of biphenyls by the Suzuki-Miyaura cross-coupling reaction. This reaction is generally performed with a phase transfer catalyst in organic solvents. Hence, any improvement of biphenyl synthesis, mainly from a view of clean reaction, is desirable.

The coupling reaction of 4-iodoanisole with phenyl boronic acid was adopted to find the optimized conditions, and the obtained data were concluded in Table 2. Since the main objective of this work was to find a clean route to synthesize biphenyls, we were interested to use DESs as reaction media. Consequently, the reactions were first screened with various hydrophilic and hydrophobic DESs at 90 °C using 0.3 mol% of the catalyst. The catalyst showed higher efficiency in hydrophilic DESs (Table 2, entries 1-8) than hydrophobic one (Table 2, entries 8-12). This might be attributed to the hydrophilic nature of the catalyst that offered more dispersion in hydrophilic DESs and thus improved its catalytic activity. Among the various hydrophilic DESs used in the reaction, DMAC:Gly afforded the highest product yield.

Under the optimized reaction solvent, the effect of using different bases like K_2CO_3 , Cs_2CO_3 , Et_3N , $NaOH$, Na_2CO_3 , KOH , and K_3PO_4 on the model reaction was examined (Table 2, entries 12-18). Although K_2CO_3 and Cs_2CO_3 revealed comparable results, we adopted K_2CO_3 as the optimal base because of its economic material benefit. Then, the reaction temperature in the range of 70-100 °C was optimized, and the results displayed that 80 °C was the best choice (Table 2, entries 19-21). Finally, the influence of catalyst loading was studied and it was found that 0.2 mol% of the catalyst was appropriate for reaction to proceed (Table 2, entries 22-24). It was found that in the absence of catalyst no reaction took place confirming the essential role of the catalyst in this reaction (Table 2, entry 25). Consequently, it was decided to use DMAC:Gly as reaction medium, K_2CO_3 as base, 0.2 mol% of the catalyst at 80 °C as the optimized reaction conditions for further experiments.

Table 2. Optimization conditions for the Suzuki-Miyaura coupling reaction using $Fe_3O_4/GO@CL-Pd$ catalyst.^a



| Entry | Catalyst (mol%) | DES | Base | T (°C) | Time (min) | Yield (%) ^b |
|-------|-----------------|-----------|-----------|--------|------------|------------------------|
| 1 | 0.3 | ChCl:Urea | K_2CO_3 | 90 | 30 | 82 |
| 2 | 0.3 | ChCl:Gly | K_2CO_3 | 90 | 30 | 88 |
| 3 | 0.3 | ChCl:CA | K_2CO_3 | 90 | 30 | 67 |
| 4 | 0.3 | ChCl:MA | K_2CO_3 | 90 | 30 | 74 |
| 5 | 0.3 | DMAC:Urea | K_2CO_3 | 90 | 30 | 86 |
| 6 | 0.3 | DMAC:Gly | K_2CO_3 | 90 | 30 | 93 |
| 7 | 0.3 | DMAC:CA | K_2CO_3 | 90 | 30 | 72 |

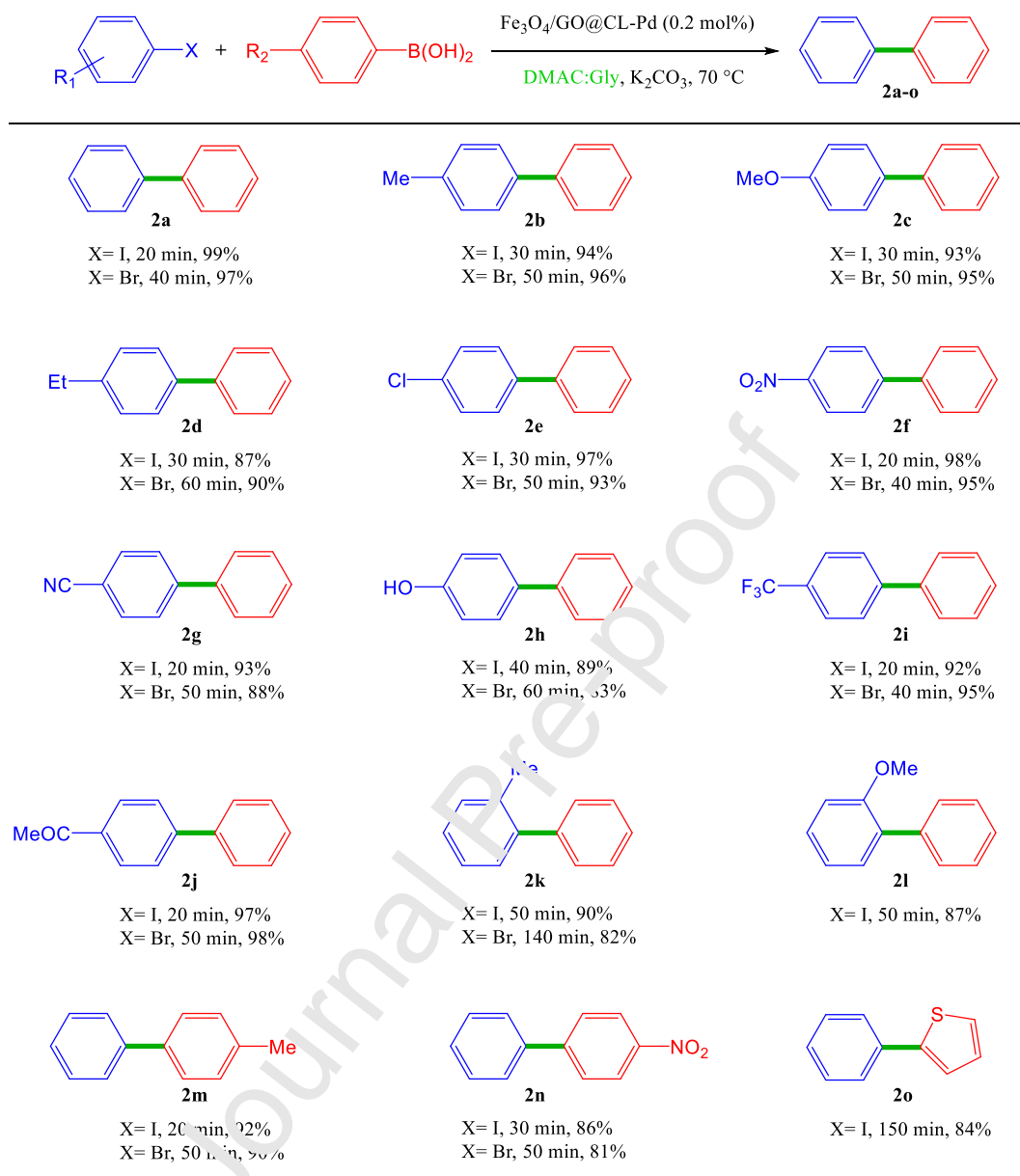
| | | | | | | |
|----|-----|----------|---------------------------------|-----|-----|----|
| 8 | 0.3 | DMAC:MA | K ₂ CO ₃ | 90 | 30 | 81 |
| 9 | 0.3 | TBAB:OA | K ₂ CO ₃ | 90 | 90 | 52 |
| 10 | 0.3 | TBAB:DA | K ₂ CO ₃ | 90 | 90 | 63 |
| 11 | 0.3 | TOMAC:OA | K ₂ CO ₃ | 90 | 90 | 59 |
| 12 | 0.3 | TOMAC:DA | K ₂ CO ₃ | 90 | 90 | 71 |
| 13 | 0.3 | DMAC:Gly | Cs ₂ CO ₃ | 90 | 30 | 95 |
| 14 | 0.3 | DMAC:Gly | Et ₃ N | 90 | 120 | 53 |
| 15 | 0.3 | DMAC:Gly | NaOH | 90 | 120 | 47 |
| 16 | 0.3 | DMAC:Gly | Na ₂ CO ₃ | 90 | 45 | 69 |
| 17 | 0.3 | DMAC:Gly | KCH | 90 | 60 | 82 |
| 18 | 0.3 | DMAC:Gly | K ₃ PO ₄ | 90 | 30 | 86 |
| 19 | 0.3 | DMAC:Gly | K ₂ CO ₃ | 100 | 30 | 94 |
| 20 | 0.3 | DMAC:Gly | K ₂ CO ₃ | 80 | 30 | 93 |
| 21 | 0.3 | DMAC:Gly | K ₂ CO ₃ | 70 | 45 | 91 |
| 22 | 0.4 | DMAC:Gly | K ₂ CO ₃ | 80 | 30 | 94 |
| 23 | 0.2 | DMAC:Gly | K ₂ CO ₃ | 80 | 30 | 93 |
| 24 | 0.1 | DMAC:Gly | K ₂ CO ₃ | 80 | 45 | 89 |
| 25 | - | DMAC:Gly | K ₂ CO ₃ | 80 | 300 | 0 |

^a Reaction conditions: 4-iodoanisole (1.0 mmol), phenyl boronic acid (1.1 mmol), base (2.0 mmol), and DES (3 mL).

^b Isolated yields.

To survey the catalytic performance of $\text{Fe}_3\text{O}_4/\text{GO}@\text{CL-Pd}$, the reaction of different aryl boronic acids and aryl halides was evaluated under the optimized reaction conditions and the data were illustrated in Scheme 2.

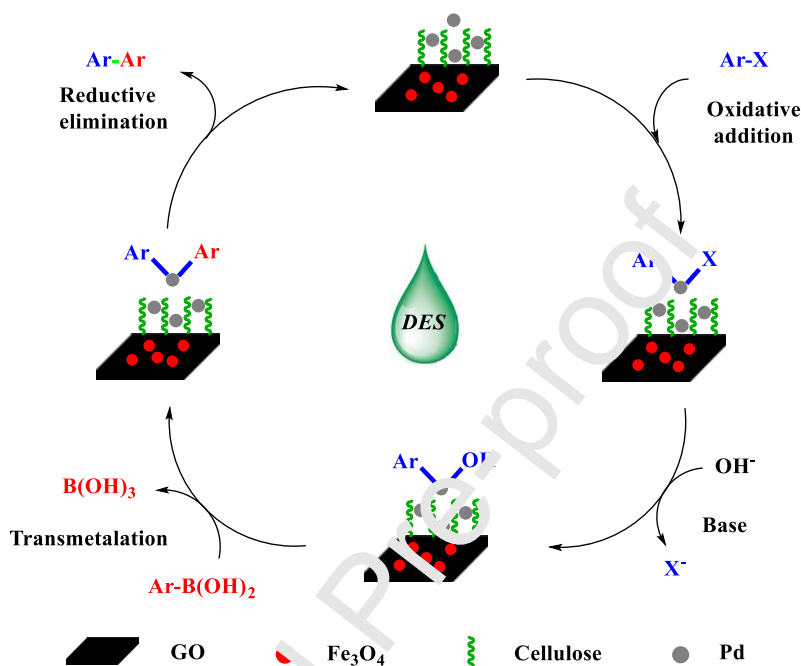
Phenyl boronic acid were efficiently reacted with some aryl iodides and bromides containing electron-donating or electron-withdrawing substituents in high yields (**2a-l**). Generally, aryl iodides revealed higher reactivity compared to aryl bromides. Moreover, the ortho-substituted aryl halides reacted slightly slower than para-substituted aryl halides owing to the steric effect. Para-substituted aryl boronic acids also coupled with iodo- and bromobenzene in excellent yields (**2m, n**). Besides, a heterocyclic aryl iodide (iodothiophene) was used and the corresponding coupling product was produced in good yield (**2o**). Notably, no product arising from the homocoupling reaction of aryl boronic acids was observed in all of the examined reactions. Overall, all the reactions were performed in the absence of organic solvents as well as other additives and high yields of different biphenyls were synthesized with a clean route.



Scheme 2. Suzuki-Miyaura coupling reaction of various aryl halides and aryl boronic acids using $\text{Fe}_3\text{O}_4/\text{GO@CL-Pd}$ catalyst. Reaction conditions: aryl halide (1.0 mmol), aryl boronic acid (1.1 mmol), K_2CO_3 (2.0 mmol), and DMAC:Gly (3 mL). All yields are isolated.

Based on the reported literature [52], a probable mechanism for the Suzuki-Miyaura coupling reaction in the presence of $\text{Fe}_3\text{O}_4/\text{GO@CL-Pd}$ was proposed in Scheme 3. At first, the oxidative addition of aryl halide to Pd nanoparticles immobilized on $\text{Fe}_3\text{O}_4/\text{GO@CL}$ took place. In the

next step, another aryl ring from aryl boronic acid attached to Pd nanoparticles through a transmetalation process. Finally, the coupling product was formed in a reductive elimination with regeneration of the catalyst.



Scheme 3. Plausible reaction mechanism for the Suzuki coupling reaction catalyzed by $\text{Fe}_3\text{O}_4/\text{GO}@CL\text{-Pd}$.

3.3. Reusability and stability of $\text{Fe}_3\text{O}_4/\text{GO}@CL\text{-Pd}$

Heterogeneous nature of $\text{Fe}_3\text{O}_4/\text{GO}@CL\text{-Pd}$ was confirmed by performing a hot filtration test for the reaction of phenyl boronic acid and 4-bromoanisole under the optimized conditions. The catalyst was magnetically isolated after 30 min and the reaction was further continued for 5 h at the same temperature of 80 °C. After removing the catalyst, no increase in the product yield was observed indicating that the catalytic process was heterogeneous.

It is essential to explore the reusability of a heterogeneous catalyst and also DES medium. In this regard, the recoverability and reusability of $\text{Fe}_3\text{O}_4/\text{GO}@CL\text{-Pd}$ and DES (DMAC:Gly) was

evaluated in the Suzuki-Miyaura reaction of phenyl boronic acid and 4-iodoanisole. The hydrophilic nature of the catalyst and DES provided a simple and clean procedure for their recovering. At the end of each reaction run, a biphasic system was formed upon addition of water and ethyl acetate to the mixture. The organic phase was collected for further product purification and analysis and the aqueous phase possessing both of the catalyst and DES was recovered by evaporating water under vacuum and recharged with fresh coupling partners and K_2CO_3 for the subsequent run. Both of the catalyst and DES were found to be efficiently reused at least five times and the product yield remained as 90% (Figure 7).

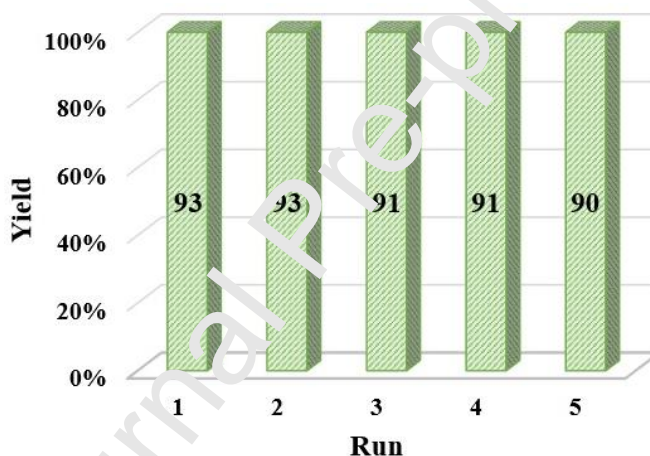


Figure 7. Recovery of $Fe_3O_4/GO@CL-Pd$ and DES (DMAC:Gly) in the Suzuki-Miyaura reaction of 4-iodoanisole and phenyl boronic acid under the optimized reaction conditions.

To verify the durability of the catalyst, $Fe_3O_4/GO@CL-Pd$ was analyzed by ICP, FT-IR, SEM, and VSM techniques after five sequential recoveries. The Pd amount of the used catalyst was measured to be 0.37 mmol.g^{-1} by ICP, which was very close to that of the fresh catalyst (0.41 mmol.g^{-1}). This revealed that $Fe_3O_4/GO@CL$ is an effective support for immobilizing Pd nanoparticles and can protect them from leaching during catalytic cycles. No significant change was found in the FT-IR spectrum, SEM image, and magnetization value of the used catalyst as

compared to the fresh one (Figure S3a-c). These results clearly confirmed the high stability and recyclability of Fe₃O₄/GO@CL-Pd.

3.4. Comparison of the catalytic performance of Fe₃O₄/GO@CL-Pd with earlier reports

To highlight the advantages of Fe₃O₄/GO@CL-Pd, its catalytic performance was compared with earlier Pd-based catalysts reported for reaction of phenyl boronic acid and 4-bromoanisole. As shown in Table 3, Fe₃O₄/GO@CL-Pd exhibits better results than other listed catalysts including high yield in less reaction time, environmental friendly and green conditions. More importantly, most of the reported catalytic systems suffer from time-consuming workup process and difficulty of separation, recovery, and reusability of the catalyst, which make them uneconomical and even unclean systems.

Table 3. Comparison of the catalytic performance of Fe₃O₄/GO@CL-Pd with other reported Pd-based catalysts in the Suzuki- Miyaura reaction of 4-bromoanisole and phenyl boronic acid.

| Catalyst (mol%) | Reaction conditions | Time | Yield (%) | Ref |
|--|--|--------|-----------|------|
| Pd-DNA-Fe ₃ O ₄ (2.8) | DES (ChCl:EG (1:2)), K ₂ CO ₃ , 80 °C | 12 h | 71.4 | [30] |
| Fe ₃ O ₄ @PFC-Pd(0) (0.24) | DES (K ₂ CO ₃ :glycerol (1:5)), 70 °C | 50 min | 93 | [33] |
| Bipyridine-Palladium (1.0) | DES (ChCl:EG (1:2)), K ₂ CO ₃ , 100 °C | 4 h | 46 | [34] |
| Pyridiniophosphine/PdCl ₂ (1.0) | DES (ChCl:glycerol (1:2)), K ₂ CO ₃ , 100 °C | 2 h | 80 | [29] |
| Palladium/Mesoionic/Carbene | DES (ChCl:CH ₂ OH) ₂ | 3 h | 90 | [31] |

| | | | | |
|--|---|----|--|-------------|
| (0.5) | (1:2)), K ₂ CO ₃ , rt | | | |
| Pd@APGO (0.23) | EtOH:H ₂ O, K ₂ CO ₃ , 6 h | 45 | | [53] |
| | 80 °C | | | |
| Cell-Sb-Pd(II) (0.3) | EtOH:H ₂ O, K ₂ CO ₃ , 1 h | 99 | | [12] |
| | 70 °C | | | |
| Fe ₃ O ₄ /GO@CL-Pd (0.2) | DES (DMAC:Gly 50 min | 95 | | [This work] |
| | (1:2)), K ₂ CO ₃ , 80 °C | | | |

4. Conclusions

In conclusion, Pd nanoparticles were supported on clicked cellulose-modified magnetite-graphene oxide nanocomposite through a facile and green reduction method without any reducing agent to afford a new hydrophilic magnetically separable Pd catalyst. The catalyst was successfully applied for the reaction of various aryl boronic acids with aryl halides in different hydrophilic and hydrophobic DESs as sustainable reaction media to achieve a clean protocol for the synthesis of biphenyls. According to the obtained results, the catalyst exhibited superior activity in hydrophilic DESs compared to hydrophobic one that may be ascribed to the better dispersion of the catalyst in hydrophilic DESs. Among various hydrophilic DESs, the mixture of dimethyl ammonium chloride and glycerol was the best one and provided excellent yield of the coupling product. Because of the very low solubility of the catalyst and DES in organic solvents, the separated aqueous phase possessing both of the catalyst and DES could be easily isolated by evaporating water and recycled five times without a discernible decrease in the product yield. This separation and recovery strategy undoubtedly provides a much cleaner route for the synthesis of biphenyls compared to other previously reported catalytic systems. Generally, the following benefits can be remarked in the present catalytic system: (a) the use of natural

cellulose as both reducing and stabilizing agents for Pd; (b) the utilization of sustainable and environmentally benign solvent (DES); (c) the recovery of the catalyst and DES in fast and easy manner; and (d) the easy separation of the catalyst by a magnet.

Declaration of competing interest

The authors declare no conflict of interest

Acknowledgements

The authors gratefully acknowledge financial support (Grant Number H/4/361) from Kharazmi University.

References

- [1] M. Fan, W.D. Wang, X. Wang, Y. Zou, Z. Long, Ultrafine Pd nanoparticles modified on azine-linked covalent organic polymers for efficient catalytic Suzuki-Miyaura coupling reaction, *Ind. Eng. Chem. Res.* 59 (2020) 12677-12685.
- [2] K. Hasan, Methyl Salicylate Functionalized Magnetic Chitosan Immobilized Palladium Nanoparticles: An Efficient Catalyst for the Suzuki and Heck Coupling Reactions in Water, *ChemistrySelect* 5 (2020) 7129-7140.
- [3] M. Kempasiddaiah, V. Kandathil, R.B. Dateer, B.S. Sasidhar, S.A. Patil, S.A. Patil, Immobilizing biogenically synthesized palladium nanoparticles on cellulose support as a green and sustainable dip catalyst for cross-coupling reaction, *Cellulose* 27 (2020) 3335-3357.
- [4] H. Hong, M. Sajjadi, J.M. Suh, K. Zhang, M. Nasrollahzadeh, H.W. Jang, R.S. Varma, M. Shokouhimehr, Palladium Nanoparticles on Assorted Nanostructured Supports: Applications for Suzuki, Heck, and Sonogashira Cross-Coupling Reactions, *ACS Appl. Nano. Mater.* 3 (2020) 2070-2103.

- [5] Z.F. Jiao, Y.M. Tian, B. Zhang, C.H. Hao, Y. Qiao, Y.X. Wang, Y. Qin, U. Radius, H. Braunschweig, T.B. Marder, X.N. Guo, X.Y. Guo, High Photocatalytic Activity of a NiO Nanodot-decorated Pd/SiC Catalyst for the Suzuki-Miyaura Cross-coupling of Aryl Bromides and Chlorides in Air under Visible Light, *J. Catal.* 389 (2020) 517-524.
- [6] E. Bulatov, E. Lahtinen, L. Kivijärvi, E. Hey-Hawkins, M. Haukka, 3D Printed Palladium Catalyst for Suzuki-Miyaura Cross-coupling Reactions, *ChemCatChem* (2020), <https://doi.org/10.1002/cctc.202000806>.
- [7] R. Jahanshahi, A. Khazaei, S. Sobhani, J.M. Sansano, γ -C₃N₄/ γ -Fe₂O₃/TiO₂/Pd: A new magnetically separable photocatalyst for visible-light-driven fluoride-free Hiyama and Suzuki-Miyaura cross-coupling reactions at room temperature, *New J. Chem.* 44 (2020) 11513-11526.
- [8] S. Supriya, G.S. Ananthnag, V.S. Shetti, B.M. Nagaraja, G. Hegde, Cost-effective bio-derived mesoporous carbon nanoparticles supported palladium catalyst for nitroarene reduction and Suzuki-Miyaura coupling by microwave approach, *Appl. Organomet. Chem.* 34 (2020) e5384.
- [9] N.Y. Baran, T. Baran, A. Menteş, Fabrication and application of cellulose Schiff base supported Pd(II) catalyst for fast and simple synthesis of biaryls via Suzuki coupling reaction, *Appl. Catal. A Gen.* 531 (2017) 36-44.
- [10] Z. Jebali, A. Granados, A. Nabili, S. Boufi, A.M.B. Rego, H. Majdoub, A. Vallribera, Cationic cellulose nanofibrils as a green support of palladium nanoparticles: catalyst evaluation in Suzuki reactions. *Cellulose* 25 (2018) 6963-6975.
- [11] Z. Lu, J.B. Jasinski, S. Handa, G.B. Hammond, Recyclable cellulose-palladium nanoparticles for clean cross-coupling chemistry, *Org. Biomol. Chem.* 16 (2018) 2748-2752.

- [12] Y. Dong, J. Bi, D. Zhu, D. Meng, S. Ming, W. Guo, Z. Chen, Q. Liu, L. Guo, T. Li, Functionalized cellulose with multiple binding sites for a palladium complex catalyst: synthesis and catalyst evaluation in Suzuki-Miyaura reactions, *Cellulose* 26 (2019) 7355-7370.
- [13] V. Kandathil, M. Kempasiddaiah, B.S. Sasidhar, S.A. Patil, From agriculture residue to catalyst support; A green and sustainable cellulose-based dip catalyst for C-C coupling and direct arylation, *Carbohydr. Polym.* 223 (2019) 115060.
- [14] P. Sun, J. Yang, C. Chen, K. Xie, J. Peng, Synthesis of a Cellulosic Pd(salen)-Type Catalytic Complex as a Green and Recyclable Catalyst for Cross-Coupling Reactions. *Catal. Lett.* 170 (2020) 1-11.
- [15] B. Wang, M. Ran, G. Fang, T. Wu, Q. Tian, L. Zheng, L. Romero-Zerón, Y. Ni, Palladium nano-catalyst supported on cationic nanocellulose-alginate hydrogel for effective catalytic reactions, *Cellulose* 27 (2020) 6995-7008.
- [16] M. Goswami, A.M. Das, Synthesis of cellulose impregnated copper nanoparticles as an efficient heterogeneous catalyst for C-N coupling reactions under mild conditions, *Carbohydr. Polym.* 195 (2018) 189-198.
- [17] Z.T. Xie, T.A. Asoh, Y. Uetake, H. Sakurai, H. Uyama, Dual roles of cellulose monolith in the continuous-flow generation and support of gold nanoparticles for green catalyst, *Carbohydr. Polym.* 247 (2020) 116723.
- [18] S.L. Cao, H. Xu, X. Li, W.Y. Lou, M. Zong, Novel Papain@Magnetic Nanocrystalline Cellulose nano-biocatalyst: a Highly Efficient Biocatalyst for Dipeptide Biosynthesis in Deep Eutectic Solvents, *ACS Sustainable Chem. Eng.* 3 (2015) 1589-1599.

- [19] M. Pudukudy, Q. Jia, Y. Dong, X. Yue, S. Shan, Magnetically separable and reusable rGO/Fe₃O₄ nanocomposites for the selective liquid phase oxidation of cyclohexene to 1,2-cyclohexane diol, *RSC Adv.* 9 (2019) 32517-32534.
- [20] J. Zhang, B. Yan, C. He, Y. Hao, S. Sun, W. Zhao, C. Zhao, Urease-Immobilized Magnetic Graphene Oxide as a Safe and Effective Urea Removal Recyclable Nanocatalyst for Blood Purification, *Ind. Eng. Chem. Res.* 59 (2020) 8955-8964.
- [21] C. Höhme, V. Filiz, C. Abetz, P. Georgopoulos, N. Scharnagl, V. Abetz, Postfunctionalization of nanoporous block copolymer membranes via Click reaction on polydopamine for liquid phase separation, *ACS Appl. Nano Mater.* 1 (2018) 3124-3136.
- [22] M. Masteri-Farahani, M. Modarres, Clicked graphene oxide as new support for the immobilization of peroxophosphotungstate: Efficient catalysts for the epoxidation of olefins. *Colloids Surf. A Physicochem. Eng. Asp.* 29 (2017) 886-892.
- [23] P.R. Boruah, A.A. Ali, S. Bishwajit, D. Sarma, A novel green protocol for ligand free Suzuki-Miyaura cross-coupling reactions in WEB at room temperature, *Green Chem.* 17 (2015) 1442-1445.
- [24] R.S. Varma, Greener and Sustainable Trends in Synthesis of Organics and Nanomaterials. *ACS Sustainable Chem. Eng.* 4 (2016) 5866-5878.
- [25] L.Y. Xie, S. Peng, F. Liu, Y.F. Liu, M. Sun, Z.L. Tang, S. Jiang, Z. Cao, W.M. He, Clean Preparation of Quinolin-2-yl Substituted Ureas in Water, *ACS Sustainable Chem. Eng.* 7 (2019) 7193-7199.
- [26] W. Tang, K.H. Row, Design and evaluation of polarity controlled and recyclable deep eutectic solvent based biphasic system for the polarity driven extraction and separation of compounds, *J. Clean. Prod.* 274 (2020) 122473.

- [27] C. Cai, Y. Wang, Y. Wang, C. Wang, F. Li, Z. Tan, Temperature-responsive deep eutectic solvents as green and recyclable media for the efficient extraction of polysaccharides from *Ganoderma lucidum*, *J. Clean. Prod.* 274 (2020) 123047.
- [28] F. Peng, Q.S. Chen, F.Z. Li, X.Y. Ou, M.H. Zong, W.Y. Lou, Using deep eutectic solvents to improve the biocatalytic reduction of 2-hydroxyacetophenone to (R)-1-phenyl-1,2-ethanediol by *Kurthia gibsonii* SC0312, *Mol. Catal.* 484 (2020) 110773.
- [29] X. Maset, A. Khoshnood, L. Sotorriós, E. Gómez-Bengoá, D.A. Alonso, D.J. Ramón, Towards DES Compatible Metallic Catalysts: Cationic Pyridinephosphine Ligands in Palladium Catalyzed Cross-Coupling Reactions, *ChemCatChem* 9 (2017) 1269-1275.
- [30] S. Chakraborty, M.H. Mruthunjayappa, K. Aruchandran, N. Singh, K. Prasad, D. Kalpana, D. Ghosh, N.S. Kotrappanavar, Facile Process for Metallizing DNA in a Multitasking Deep Eutectic Solvent for Ecofriendly C-C Coupling Reaction and Nitrobenzene Reduction, *ACS Sustainable Chem. Eng.* 7 (2019) 14225-14235.
- [31] X. Maset, B. Saavedra, N. Gonzalez-Gallardo, A. Beaton, M.M. León, R. Luna, D.J. Ramón, G. Guillena, Palladium Mesoionic Carbene Pre-catalyst for General Cross-Coupling Transformations in Deep Eutectic Solvents, *Front. Chem.* 7 (2019) 700.
- [32] M. Heidari, M. Faravi, R. Nabid, R. Sedghi, S.E. Hooshmand, Novel palladium nanoparticles supported on β -cyclodextrin@graphene oxide as magnetically recyclable catalyst for Suzuki-Miyaura cross-coupling reaction with two different approaches in bio-based solvents, *Appl. Organomet. Chem.* 33 (2019) e4632.
- [33] A. Salamatmanesh, A. Heydari, H.T. Nahzomi, Stabilizing Pd on magnetic phosphine-functionalized cellulose: DFT study and catalytic performance under deep eutectic solvent assisted conditions, *Carbohydr. Polym.* 235 (2020) 115947.

- [34] B. Saavedra, N. González-Gallardo, A. Meli, D.J. Ramón, A Bipyridine-Palladium Derivative as General Pre-Catalyst for Cross-Coupling Reactions in Deep Eutectic Solvents, *Adv. Synth. Catal.* 361 (2019) 3868-3879.
- [35] Z. Xu, C. Gao, Aqueous Liquid Crystals of Graphene Oxide, *ACS Nano* 5 (2011) 2908-2915.
- [36] E. Kazemi, A.M.H. Shabani, S. Dadfarnia, A. Abbasi, M.R.V. Rashidian, A. Behjat, Development of a novel mixed hemimicelles dispersive micro solid phase extraction using 1-hexadecyl-3-methylimidazolium bromide coated magnetic graphene for the separation and preconcentration of fluoxetine in different matrices before its determination by fiber optic linear array spectrophotometry and mode-mismatched thermal lens spectroscopy, *Anal. Chim. Acta* 905 (2016) 85-92.
- [37] G. Mangiante, P. Alcouffe, B. Burdick, M. Gaborieau, E. Zeno, M. Petit-Conil, J. Bernard, A. Charlot, E. Fleury, Green nondegrading approach to alkyne-functionalized cellulose fibers and biohybrids thereof: synthesis and mapping of the derivatization, *Biomacromolecules* 14 (2013) 254-263.
- [38] P. Makoś, A. Słupek, J. Cębicki, Hydrophobic deep eutectic solvents in microextraction techniques-A review, *Microchem. J.* 152 (2020) 104384.
- [39] H. Qin, X. Hu, J. Wang, H. Cheng, L. Chen, Z. Qi, Overview of Acidic Deep Eutectic Solvents on Synthesis, Properties and Applications. *Green Energy Environ.* 5 (2020) 8-21.
- [40] H. Shekaari, I. Ahadzadeh, S. Karimi, Understanding solvation behavior of glucose in aqueous solutions of some deep eutectic solvents by thermodynamic approach, *J. Mol. Liq.* 289 (2019) 111000.

- [41] M. Masteri-Farahani, M. Ghahremani, Surface functionalization of graphene oxide and graphene oxide-magnetite nanocomposite with molybdenum-bidentate Schiff base complex, *J. Phys. Chem. Solids*. 130 (2019) 6-12.
- [42] A. Aliyari, M. Alvand, F. Shemirani, Modified surface-active ionic liquid-coated magnetic graphene oxide as a new magnetic solid phase extraction sorbent for preconcentration of trace nickel, *RSC Adv.* 6 (2016) 64193-64202.
- [43] Q. Zhang, H. Su, J. Luo, Y. Wei, "Click" magnetic nanoparticle-supported palladium catalyst: a phosphine-free, highly efficient and magnetically recoverable catalyst for Suzuki-Miyaura coupling reactions, *Catal. Sci. Technol.* 3 (2013) 235-243.
- [44] P. Sharma, J. Rathod, A. P. Singh, P. Kumar, Y. Sasun, Synthesis of heterogeneous Ru(II)-1,2,3-triazole catalyst supported over SBA-15: application to the hydrogen transfer reaction and unusual highly selective 1,4-disubstituted triazole formation *via* multicomponent click reaction, *Catal. Sci. Technol.* 8 (2018) 3246-3259.
- [45] S. Sankar, N. Watanabe, G.M. Arulkumar, B.N. Nair, S.G. Sivakamiammal, T. Tamaki, T. Yamaguchi, Electro-oxidation competency of palladium nanocatalysts over ceria-carbon composite supports during alkaline ethylene glycol oxidation, *Catal. Sci. Technol.* 9 (2019) 493-501.
- [46] E. Doustkhah, S. Rostamnia, Covalently bonded sulfonic acid magnetic graphene oxide: Fe₃O₄@GO-Pr-SO₃H as a powerful hybrid catalyst for synthesis of indazolophthalazinetriones, *J. Colloid Interface Sci.* 478 (2016) 280-287.
- [47] S. Farhadi, M. Hakimi, M. Maleki, 12-Molybdophosphoric acid anchored on aminopropylsilanized magnetic graphene oxide nanosheets (Fe₃O₄/GrOSi(CH₂)₃

NH₂/H₃PMo₁₂O₄₀): a novel magnetically recoverable solid catalyst for H₂O₂-mediated oxidation of benzylic alcohols under solvent-free conditions, RSC Adv. 8 (2018) 6768-6780.

[48] H.Y. Xu, B. Li, T.N. Shi, Y. Wang, S. Komarneni, Nanoparticles of magnetite anchored onto few-layer graphene: A highly efficient Fenton-like nanocomposite catalyst, J. Colloid Interface Sci. 532 (2018) 161-170.

[49] Y. Xing, J. Han, L. Wang, C. Li, J. Wu, Y. Mao, L. Ni, Y. Wang, Fabrication of dendrimeric phenylboronic acid-affinitive magnetic graphene oxide nanoparticles with excellent adsorption performance for separation and purification of Horseradish peroxidase, New J. Chem. 44 (2020) 5254-5264.

[50] Y. Shen, X. Bo, Z. Tian, Y. Wang, X. Guo, M. Xie, F. Gao, M. Lin, X. Guo, W. Ding, Fabrication of Highly Dispersed/Active Ultrafine Pd Nanoparticles Supported Catalyst: a Facile Solvent-free In-situ Dispersion/Reduction Method, Green Chem. 19 (2017) 2646-2652.

[51] S. Sadjadi, M. M. Heravi, M. Malmir, Pd(0) nanoparticle immobilized on cyclodextrin-nanosponge-decorated Fe₂O₃@SiO₂ core-shell hollow sphere: An efficient catalyst for C-C coupling reactions, J. Taiwan Inst. Chem. Eng. 86 (2018) 240-251.

[52] E. Niknam, F. Panahi, A. Zhalafi-Nezhad, Immobilized Pd on a NHC functionalized metal-organic framework MIL-101(Cr): an efficient heterogeneous catalyst in Suzuki-Miyaura coupling reaction in water, Appl. Organomet. Chem. 34 (2020) e5470.

[53] V.B. Saptal, M.V. Saptal, R.S. Mane, T. Sasaki, B.M. Bhanage, Amine-Functionalized Graphene Oxide-Stabilized Pd Nanoparticles (Pd@APGO): A Novel and Efficient Catalyst for the Suzuki and Carbonylative Suzuki-Miyaura Coupling Reactions, ACS Omega 4 (2019) 643-649.

CRedit author statement

Mahsa Niakan: Data Curation, Investigation, Writing - Original Draft

Majid Masteri-Farahani: Supervision, Writing - Review & Editing

Sabah Karimi: Investigation, Writing - Original Draft

Hemayat Shekaari: Writing - Review & Editing

Journal Pre-proof

Declaration of interests

The authors declare that they have no known competing financial interests or personal relationships that could have appeared to influence the work reported in this paper.

The authors declare the following financial interests/personal relationships which may be considered as potential competing interests:

Highlights

- Cellulose-modified magnetite-graphene oxide nanocomposite was utilized for immobilization of Pd nanoparticles.
- The prepared material served as a catalyst for the preparation of biphenyls through the Suzuki-Miyaura coupling reaction.
- Various hydrophilic and hydrophobic deep eutectic solvents (DESs) were used as reaction media.